Journal of South American Earth Sciences, Vol. 4, No. 1/2, pp. 13–24, 1991
Printed in Great Britain

0895-9811/91 $3.00 + 0.00

Seismicity and tectonic deformation in the Eastern Cordillera and the sub-Andean zone of central Peru

L. DORBATH[1,2], C. DORBATH[1,2], E. JIMENEZ[2], and L. RIVERA[2]

[1]ORSTOM, 213 Rue La Fayette, 75480 Paris Cedex 10, France; [2]Ecole et Observatoire de Physique du Globe de Strasbourg, 5 Rue René Descartes, 67084 Strasbourg Cedex, France

(*received April 1990; accepted January 1991*)

Abstract—A microearthquake survey, conducted in 1985 on the Eastern Cordillera and the sub-Andean zone of central Peru, provides a precise description of the crustal seismicity of this region. The activity is mainly concentrated in the eastern foot of the high chain and defines a fault that strikes NW-SE and dips steeply to the west. Focal mechanisms show mainly inverse dip-slip solutions, and hypocenter depths reach 35 km. The seismic belt follows the border between the Eastern Cordillera and the lowlands in the south and is separated from the Cordillera north of 11°S, in the most seismically active part. The amount of shortening, deduced from a study of major earthquakes that have occurred in the region, is about 4 mm/year. We propose a process of shortening along this active tectonic fault involving a large part of the crust, if not its entirety. The intense seismicity on this fault is associated with the uplift of the Andes and their widening toward the north.

Resumen—Un estudio microsísmico, desarrollado en 1985 en la Cordillera Oriental y la zona sub-Andina del Perú central, provee una descripción precisa de la sismicidad cortical en esta región. La actividad está esencialmente concentrada en el borde Este de la cadena, y define una falla NO-SE, de fuerte pendiente y buzando al Oeste. Los mecanismos focales son en su mayoría inversos y las profundidades de los hipocentros alcanzan 35 km. En su parte sur, la sismicidad coincide con el límite entre la Cordillera Oriental y el Piedemonte; en cambio, al norte de 11°S, en la parte más activa, dicho límite cambia de dirección mientras que la sismicidad continua en la misma línea. El acortamiento, asociado a los terremotos más importantes occuridos en esta zona, es de 4 mm/año aproximadamente. Se propone un proceso de acortamiento a lo largo de la falla antes mencionada involucrando toda la corteza o al menos una gran parte de ella. La intensa sismicidad asociada a esta falla es testigo del levantamiento de los Andes y de su ensanchamiento hacia el norte.

INTRODUCTION

THE SHALLOW SEISMICITY of the Andean region is mainly concentrated within two belts parallel to the chain on both sides of it (Fig. 1). To the west, the first belt underlies the contact between the subducted Nazca plate and the South American plate. The second belt of seismic activity lies within the overriding continental plate to the east of the chain, in the sub-Andean region.

Although the seismic activity is predominant in these two belts, several events occur within the high chain. Most of them reveal normal faulting. The greatest intraplate event in recent time in Peru was the 1946 Ancash earthquake. Observations on the scarps produced by this event (Silgado, 1951) as fault-plane solutions (Doser, 1987, Deverchère *et al.*, 1989) show that normal faulting occurred on a plane roughly parallel to the Andes and dipping 45° to the west. Spectacular normal faults border the western flank of the Cordillera Blanca of central Peru (Dalmayrac and Molnar, 1981), and a microearthquake survey in the area indicates a component of extension perpendicular to the range (Deverchère *et al.*, 1989). Extension is documented in several other localities in the high Andes (Sébrier *et al.*, 1985, Sébrier *et al.*, 1988).

Although normal faulting appears to be the prevalent style of deformation throughout much of the high Andes, thrust faulting has been reported in some parts, particularly in the Eastern Cordillera of central Peru near the Huaytapallana range. Two events occurred in July and October 1969 and produced surface breaks along two segments of the Huaytapallana fault, which crops out at a mean elevation of 4800 meters above sea level (Blanc *et al.*,

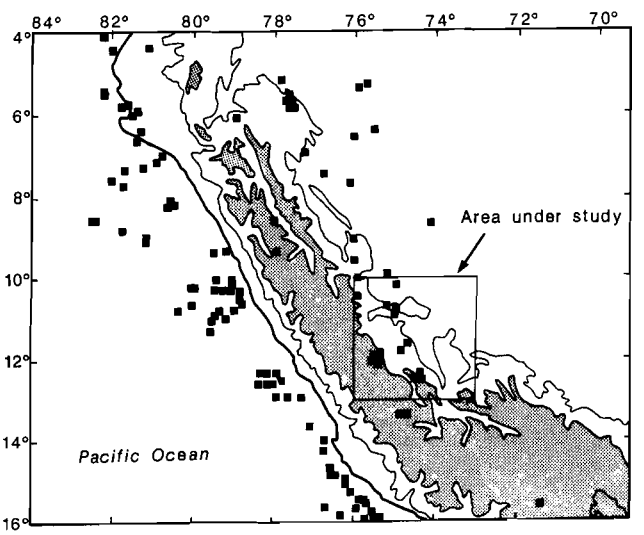

Fig. 1. Shallow seismicity of Peru from ISC bulletin (most reliable solutions) between 1965 and 1983. Shaded area is above 3000 meters elevation.

Address all correspondence and reprint requests to: Dr. C. Dorbath, EOPGS, 67084 Strasbourg Cedex, France (Telephone: 33-88-416300; Fax: 33-88-616747).

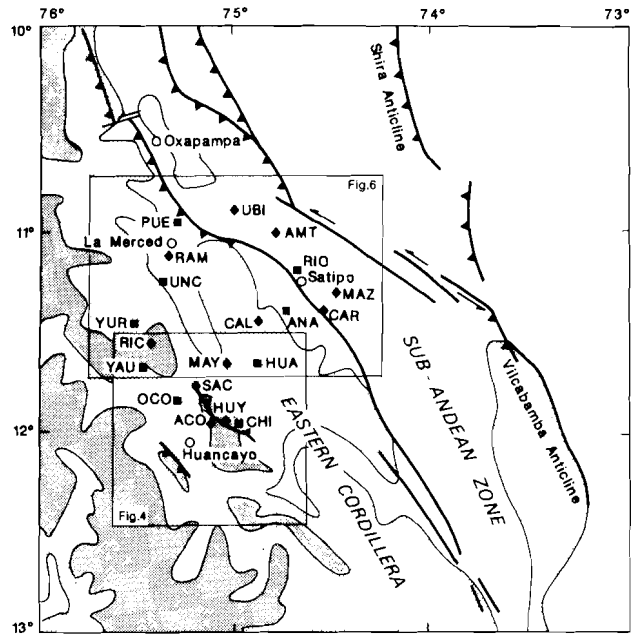

Fig. 2. Tectonic and topographic map of the area under study. Lightly shaded regions are above 2000 meters elevation, and dark ones above 4000 meters. Seismic temporary stations are shown by squares (digital) or diamond-shaped (analogic) symbols. Thick solid lines are faults after Mégard (1978). Open circles are towns.

1983). Microtectonic study of the scarp and fault-plane solutions show reverse faulting with some left-lateral strike-slip motion on planes dipping about 50° to the east (Philip and Mégard, 1977; Suarez *et al.*, 1983).

From May 13 to June 12, 1980, a temporary network of portable seismographs was operated in the high plateaux and Eastern Cordillera of the Central Andes of Peru, in the vicinity of Huancayo (Suarez *et al.*, 1990). Only a few events occurred in the crust beneath the network, except along the Huaytapallana fault. Most of the crustal microearthquakes were located to the east, in the western part of the sub-Andean region, at large distances from the network, and therefore their focal depths are poorly constrained. Most of the sufficiently well located events occurred at mid-crustal depth between 15 and 25 km, and a significant number (10%) at depths greater than 35 km and up to 55 km. On the other hand, Suarez *et al.* (1983) determined the focal depths of large intracontinental earthquakes using synthetic waveforms and concluded that they range from 10 km to 38 km. These two sets of data suggest that the lower crust and possibly the uppermost mantle are involved in brittle deformation. Fault-plane solutions of events in the sub-Andean region show reverse faulting on steeply west-dipping planes striking NW-SE. This style of deformation would reflect the underthrusting of the Brazilian Shield under the Eastern Cordillera.

The coexistence of normal faulting in the high parts of the chain and reverse faulting on both sides led Suarez *et al.* (1983) to propose a model of construction of the Andes by eastward migration of thrust faulting involving the whole crust, resulting in crustal thickening and uplift. The gravitational body forces acting on the region of high topography and the buoyancy forces caused by the crustal root balance the horizontal compressive stress applied on the sides.

The crustal seismic activity within the Eastern Cordillera and its eastern margin is quite low compared to the subduction zone. Very few events are likely to give reliable fault-plane solutions. Moreover, the hypocentral locations determined by the International Seismological Center (ISC) are not accurate enough to produce precise information about the position of active faulting due to the lack of local seismological stations and the uneven distribution of distant ones. This is particularly true for focal depths. In order to achieve such information, we installed a temporary network of portable stations in the Eastern Cordillera and western side of the sub-Andean zone.

GEOLOGIC AND TECTONIC SETTING

The array lies over three morphostructural zones: the Mantaro Basin, which is the extension of the Altiplano to the north, the Eastern Cordillera, and the sub-Andean zone (Figs. 2 and 4). The Mantaro Basin and its tectonic units were described in a previous paper (Dorbath *et al.*, 1990).

The Eastern Cordillera is an Andean anticlinorium, about 100 km wide, bordered on both sides by faults. Outcrops are mainly crystalline Precambrian and early Paleozoic rocks. However, large areas show late Paleozoic and Mesozoic cover; the latter has been folded during the Andean orogeny, principally during the Late Cretaceous and late Eocene, and faulted during the Miocene (Audebaud *et al.*,1973; Mégard, 1978). The most recent deformations correspond to a ENE-WSW compression along the active Huaytapallana fault (Philip and Mégard, 1977; Dorbath *et al.*, 1990). In the area under study, the Eastern Cordillera culminate in the Huaytapallana range at more than 5500 meters. The elevation rapidly decreases toward the east down to 500 meters in the sub-Andean zone. The boundary between the Eastern Cordillera and the sub-Andean region is generally shown to be the zone of west-dipping reverse faults that follows the 2000-meter contour line (Fig. 2).

The sub-Andean Zone is a 200-km-wide belt between the Eastern Cordillera and the stable Brazilian Shield. It consists of sedimentary rocks of Paleozoic to Quaternary age, deposited without unconformities up to the Paleogene, and possibly up to the mid-Pliocene (Sébrier *et al.*, 1988). The thickness of this sedimentary cover is poorly known in the region but, more to the north, thicknesses up to 10 km have been reported from seismic reflection studies (Pardo, 1982); it narrows and thins from north to south. Since mid-Pliocene time it has been folded, and associated steep west-dipping reverse faults developed,

some of which are thought to affect the basement (Audebaud *et al.*, 1973). This compressive regime of deformation continues up to now.

The western part of the sub-Andean zone, 30 km to 40 km wide, is formed by NNW-SSE isopach cylindrical folds, frequently overturned to the east. The anticlines are generally flanked by west-dipping thrusts. This part of the sub-Andean region is limited to the east by a major reverse fault, first described by Hamm and Herrera (1963) (Fig. 2). Its vertical throw could reach 5000 meters. To the east, the intensity of tectonic deformation rapidly decreases, and the distance between two successive folds increases. The Shira and Vilcabamba anticlines are the main features. They are limited to the east by west-dipping faults. Toward the Brazilian Shield, some isolated anticlines appear, separated by large flat synclines.

The total amount of shortening is not well controlled, due to the absence of seismic profiling. In northern Peru, oil exploration data led Pardo (1982) to interpret the sub-Andes as a thin-skinned fold-and-thrust belt. There, the shortening since mid-Pliocene times is about 50 km. This value is probably an upper limit in central Peru.

DESCRIPTION OF THE NETWORK AND DATA ANALYSIS

Twenty short-period portable autonomous seismic stations were operated during July and August 1985, equally distributed over the Eastern Cordillera and the sub-Andean region (Fig. 2, Table 1). We used 11 Sprengnether MEQ-800 seismographs with Mark Product L4C vertical seismometers (1hz natural frequency); the seismic signals were recorded on smoked paper at a speed of 60 mm/mn. The internal clock supplied a time mark every second. Drifts of the internal clocks were checked every 48 hours, by recording time signal transmitted by WWV. Clock drifts were linear and smaller than 0.05 s/day. We also checked that within a day the non-linear variations were inferior to the reading errors. The 9 other stations were digital 3-component magnetic tape Geostras recorders, developed at the IPG Strasbourg, with Mark Products L22 seismometers (2 hz natural frequency). The timing system was provided by a crystal clock synchronized by radio signal from the Argentina transmitter of the Omega system.

A careful search of sites offering good recording conditions, *e.g.*, quarries, closed mine galleries, allowed the set of gains at 84 db and 90 db for the stations located on the Eastern Cordillera and from 78 db to 90 db for the ones in the sub-Andean region, despite the scarcity of outcrops and the abundance of vegetation in the lowlands. A filter with the band pass upper edge limit set at 30 hz was used.

The geographic coordinates and elevation of the stations on the Eastern Cordillera were determined using topographic maps at scales of 1/25,000 and 1/100,000 from the Instituto Geografico Militar del Peru; those in the sub-Andean region were determined using maps at scales of 1/25,000 and 1/10,000 from the Ministerio de Agricultura and unpublished army documents. The errors in locations are estimated to be 250 meters at the most.

The uncertainties in arrival times depend on the type of station. For the smoked paper analog record-

Table 1. Temporary network.

Code	Name	Latitude	Longitude	Elevation (meters)	Type	Velocity Model (Table 2)
ACO	Acopalca	11° 58.93S	75° 05.91W	3933	MEQ	M
AMT	Amauta	10° 59.07S	74° 46.57W	590	MEQ	J
ANA	Santa Viviana	11° 21.41S	74° 43.10W	1200	GEO	J
CAL	Calabasa	11° 30.45S	74° 49.65W	2000	MEQ	J
CAR	Caracol	11° 24.46S	74° 30.76W	880	MEQ	J
CHJI	Chilifruta	11° 59.52S	74° 57.80W	3790	GEO	M
HUA	Huanca	11° 40.56S	74° 53.15W	4140	GEO	M
HUY	Huaytapallana	11° 57.67S	75° 02.54W	4325	MEQ	M
MAY	Maraynioc	11° 39.66S	75° 01.30W	3850	MEQ	M
MAZ	Mazamari	11° 17.88S	74° 27.43W	560	MEQ	J
OCO	Sta Rosa de Ocopa	11° 51.50S	75° 16.65W	3543	GEO	M
PUE	Pueblo Pardo	10° 56.36S	75° 17.61W	730	GEO	J
RAM	San Ramon	11° 07.08S	75° 20.17W	700	MEQ	J
RIC	Ricran	11° 34.56S	75° 26.54W	4510	MEQ	M
RIO	Rio Negro	11° 11.91S	74° 40.58W	750	GEO	J
SAC	Sacsacancha	11° 46.73S	75° 12.02W	4350	MEQ	M
UBI	Ubiriqui	10° 52.72S	75° 00.35W	810	MEQ	J
UNC	Mina San Vincente	11° 17.88S	75° 20.58W	2330	GEO	J
YAU	Yauli	11° 40.99S	75° 29.12W	3500	GEO	M
YUR	Yuracmayo	11° 27.62S	75° 31.40W	3620	GEO	M

ers, the use of a magnifying lens allows a precision of 0.05 mm, and thus the uncertainties in P-wave arrival times are less than 0.1 second. For S-waves, these uncertainties are of course greater; from comparison with digital records and an *a posteriori* control, we estimate S-wave arrival time uncertainties to be about 0.5 second. Digital records were read on a microcomputer, and we consider the uncertainties in arrival times to be reduced by a factor of two with respect to the analog records.

The earthquakes were located using the computer program HYPOINVERSE (Klein, 1978), modified to compensate for the differences in station elevation, because our network ranged from less than 1000 meters above sea level to more than 4500 meters above sea level.

The velocity structure in central Peru is poorly known. Refraction studies were carried out in southern Peru and northern Bolivia (Ocola *et al.*, 1971; Ocola and Meyer, 1973), in southern Colombia (Meissner *et al.*, 1976), and in Ecuador (Durand, 1987). Several tests were performed on selected earthquakes to determine the dependence of hypocentral locations on the choice of velocity structure. As in previous studies (*e.g.*, Grange, 1983; Suarez *et al.*,1990), we found that epicentral coordinates do not strongly depend on the velocity model and that focal depth is the parameter most sensitive to structural changes. Typical values are 2 to 4 km for changes in epicentral coordinates and 4 to 8 km for depth variations. As expected, the earthquakes that show the smaller hypocentral changes are events inside the network or close to it. The V_P/V_S ratio was determined from Wadati plot to be 1.73; this value has been used throughout the data treatment.

Two different structures have been used to simulate the increase in crustal thickness from the sub-Andean region to the high chain. The model in Table 2 was adopted to locate all the events because it produces the smallest root mean square values of travel time residuals. This model is quite comparable to those established in southern Colombia and Ecuador and to that used by Grange *et al.* (1984). Station time corrections were applied to all arrival times. These delays were obtained from a previous location by averaging the residuals of a selection of well located events at each station. However, the delays were small and had only a weak influence on the final locations.

Four hundred and eighty crustal events were located that meet the following criteria: 6 or more phases including one S; RMS less than 0.50 second; conditioning number (ratio of the largest to the smallest singular values of the matrix of partial derivatives) less than 100. The locations of these events with various velocity models differ by less than 10 km even when they are located outside the array. These events form a set of reliable hypocenters labeled RH. Among this set, 215 events meet more restrictive criteria which insure that they are very well located: 8 or more phases including at least one S arrival time; RMS less than 0.3 second; maximum azimuthal aperture from the epicenter without station lesser than 300°; epicentral distance to the nearest station less than calculated focal depth. This set of the most reliable hypocenters is labeled MRH. 4962 phases were used to compute RH hypocenters parameters, and 2531 for MRH, that is 12 phases on average for each event from this last set.

Table 2. Velocity models.

Mountain		Jungle	
km	km/s	km	km/s
0	5.8	0	5.8
15	6.2	12	6.2
30	6.8	25	6.8
50	8.0	40	8.0

The focal depth is the parameter that generally displays the poorest resolution. The use of S phases guarantees a good control on depths. It is worth noting that only 7% and 2%, respectively, of the RH and MRH focus were computed using only one S arrival time, and 66% and 87%, respectively, were determined using 3 or more S phases. 90% of the events have standard errors on depth less than 4.5 km and 3.5 km for RH and MRH sets, respectively. Nevertheless, focal depth accuracy strongly depends on the relative positions of hypocenters and seismic network. Figure 3 shows some typical RMS variations with depth for an event near the Huaytapallana cordillera (Fig. 3a), two events in the sub-Andean zone inside the array (Figs. 3b and 3c) and another one away from the network (Fig. 3d). The half-width of the curves where $RMS = 1.5\ RMS_{min}$, arbitrarily chosen as the uncertainty on the depth, varies from 2 to 2.5 km for focus which lies inside the array or very close to it, to more than 5 km far outside. Finally, we estimate that the precision of the location is about 3 km in epicentral position and 5 km in depth for the events inside the array or in its vicinity, that is generally belonging to the MRH set, and twice these estimations far from the network.

The magnitudes were computed from the duration of the coda using the relation established for Alaska (Klein,1978), already used by Grange *et al.* (1984) in southern Peru.

SEISMICITY OF THE EASTERN CORDILLERA AND SUB-ANDEAN ZONE

Huancayo Basin and Eastern Cordillera (Fig. 4)

A detailed account of the seismicity of the Mantaro Basin and the Huaytapallana fault has already been published in previous papers (Suarez *et al.*,1990; Dorbath *et al.*,1990), summarized briefly here.

Along the Huaytapallana fault in the Eastern Cordillera, the depths of the foci are less than 10 km. Reverse faulting occurs on a plane dipping 50° to the east in agreement with the mechanisms and the

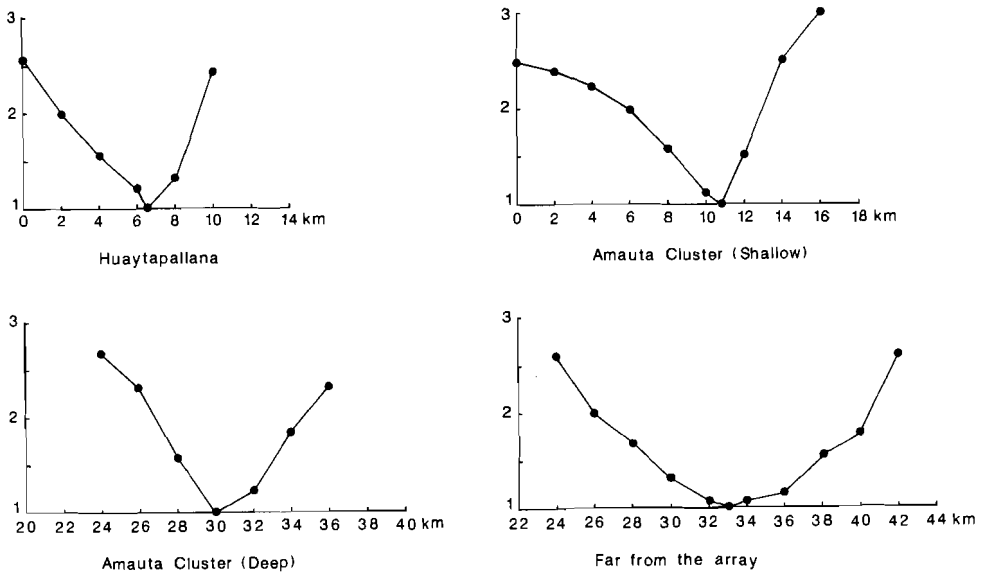

Fig. 3. Variations of RMS with depth for some typical events.

neotectonic observations of the July 24 and October 1, 1969 large earthquakes. Precise relative determination of hypocenters shows clustering around gaps that were not broken during the 1969 crisis, so that earthquakes of similar sizes may be expected in the future in these locations. During the 1985 survey, another cluster appeared in the Eastern Cordillera near Pampas. These events lie outside the seismic array, and, therefore, their depths are not well resolved; however, they probably do not exceed 15 km. Focal mechanisms are comparable to those of the Huaytapallana fault zone.

On the other side of the Mantaro Basin, seismic activity has been found on the eastern flank of the Western Cordillera. The spatial distribution of hypocenters agrees with field observations of the west-dipping Altos del Mantaro fracture zone separating the Western Cordillera from the Mantaro Basin (Mégard, 1978; Blanc, 1984). In other parts of the high chain, the activity is sparse.

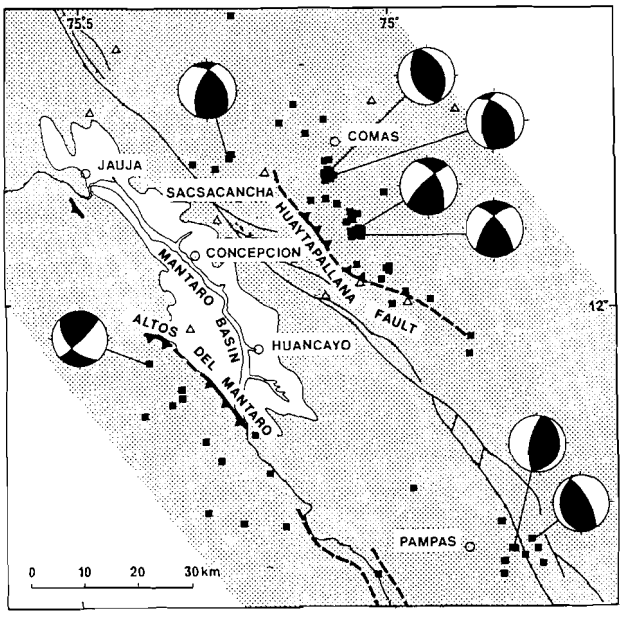

Fig. 4. Seismicity of the Mantaro basin and Eastern Cordillera (closed squares) and focal mechanisms of selected events from Dorbath *et al.* (1990). Open triangles are seismic stations, open circles are towns. Shaded regions are above 3500 meters elevation. Solid and segmented lines are faults after Mégard (1978) and Blanc (1984).

Sub-Andean Zone

Figure 5 shows the epicenters of all the events from the RH set. Figure 6 shows only the central part of Fig. 5 where hypocenter parameters are better constrained, because events are inside the network or very close to it, and where focal mechanisms may have been produced; nearly all of these events belong to the MRH set.

East of the Eastern Cordillera, a belt of intense seismic activity is in evidence; it follows the general strike of the chain. It is noteworthy that the activity is much more abundant between 10.5°S and 11.5°S. This pattern is not an artifact due to the network geometry, and the criteria events have to be fulfilled in order to be selected. This is obvious south of 11.5°S, where the seismicity rapidly decreases, although several stations are close to it. In the same latitude range the topography, outlined by the 2000-meter contour line, and the different fault systems do not follow a straight trend. Thus the seismic activity concentrates where the eastern border of the Andes is sharply deflected.

South of about 11.5°S, the epicenters lie west of the fault that marks the border of the Eastern Cordillera, in agreement with its westward dip recognized on the field. Between 11.5°S and 10.8°S the epicenters lying to the southwest of the same fault define a narrow weak band of activity following and even accentuating the shift of the structures; it runs nearly east-west just south of 11°S. More to the north, very few events may define a band turning back to the N140° azimuth as in the southern part. Therefore, the fault that marks the boundary between the Andean range and the sub-Andean zone, recognized

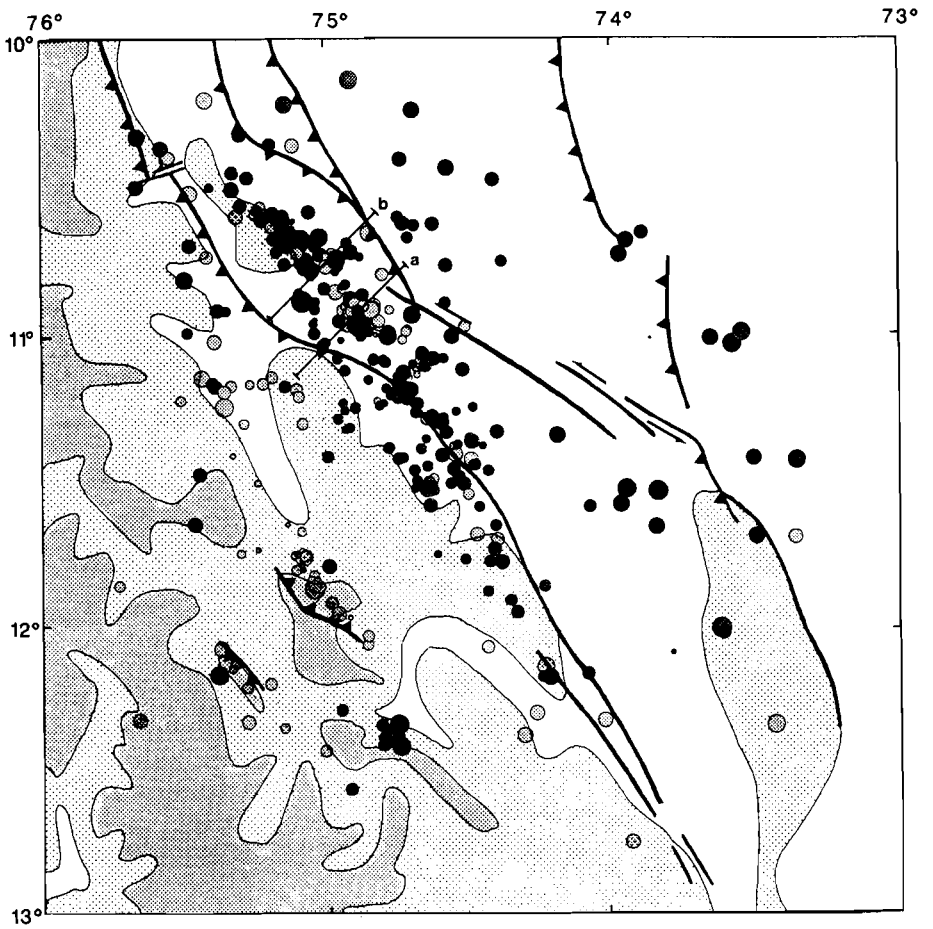

Fig. 5. Seismicity of the sub-Andean region of central Peru on a topographic and tectonic frame (see Fig. 2). Depth of events is indicated by increasing shades: 0–12.5 km, 12.5–22.5 km, >22.5 km. Also shown are the locations of the cross-sections on Fig. 7.

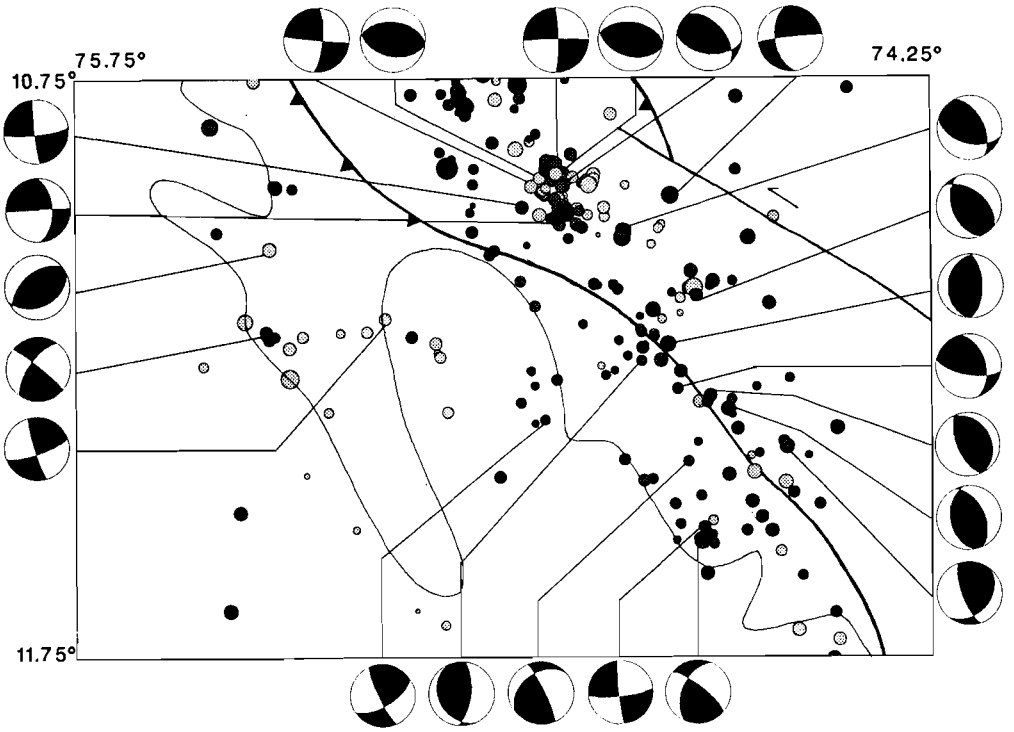

Fig. 6. Central part of Fig. 5 with individual focal mechanisms deduced from the inversion of polarities (Rivera and Cisternas, 1990).

by geologists, is an active feature, even if this activity is not as intense as that observed more to the east. The depths of the hypocenters do not exceed 25 km, which is relatively shallow for the region, as will be seen later on. Only a few focal mechanisms have been constructed. Taking as fault plane the nodal plane striking the same direction as the general trend of the seismicity, almost all of them are pure sinistral strike-slip faulting along the offset; a strong dip-slip inverse component is present elsewhere. Thus, from its geometry and faulting type, this fault appears to be formed by two parallel segments, where inverse faulting is dominant and offset by a sinistral wrench fault where the seismicity is more superficial.

As already asserted in a previous paper (Dorbath *et al.*, 1986) describing only a subset of all events, a major seismically active zone exists beyond the boundary between the Eastern Cordillera and the sub-Andean hills, within the sub-Andes. The epicenters define an elongated zone about 120 km long and 20 km wide, striking N140°. It includes several clusters where activity is very high, like that which we called the Amauta cluster in the first paper. To the south, this seismic belt joins with that associated with the fault bounding the Eastern Cordillera at about 11.5°S. Focal mechanisms are dominantly inverse dip-slip faulting, but some of them are sinistral strike-slip (Fig. 6).

The uncertainty of the hypocenters parameters do not allow a fine description of each of these clusters, particularly to the north. A cross-section across the Amauta cluster (see Fig. 5) is shown on Fig.7a. Depths of events range from 5 to 35 km; the activity mainly occurs within the hanging block of the high-dipping fault which Ham and Herrera (1963) described as separating the western part of the sub-Andean zone, where tectonic deformation is very strong, from its eastern part, where tectonic deformation is weaker. The dip of this fault is about 45°; Ham and Herrera (1963) measured more than 50° at the surface. On the same cross-section a linear dense concentration of hypocenters from 5 to 20 km suggests an antithetic fault steeply dipping eastward. The result of inverse dip-slip movement along these two faults should be the uplift of the prism bounded by them. Unfortunately, no precise topographic map is available for this area, but this style of deformation has been documented in other parts of the sub-Andes, *e.g.*, in northern Argentina, where the absence of vegetation allows direct observation of the faults (Jordan *et al.*, 1983). Another cross-section (Figs. 5 and 7b) displays a quite similar pattern relative to the trace of the fault mapped by Ham and Herrera (1963).

Therefore, the overall seismicity occurring in the western sub-Andes can be associated with two west-dipping fault systems: *(i)* the fault system that marks the boundary between the high chain and the sub-Andean region, active all along this boundary and more active south of 11°S; and *(ii)* the fault system that divides the sub-Andean region between a strongly deformed belt to the west and a gently

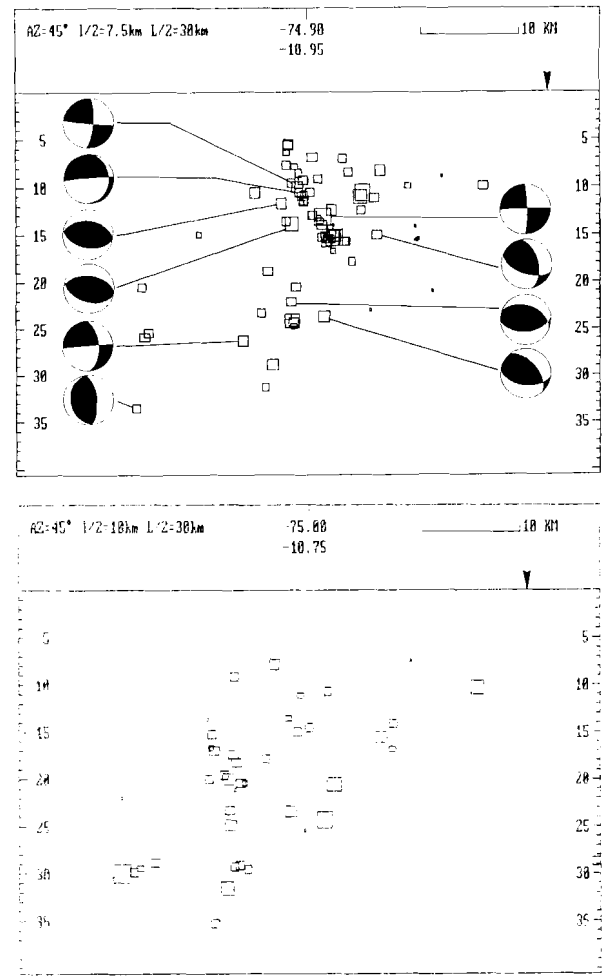

Fig. 7. a) Cross-section through the Amauta cluster following the azimuth N45°. The arrow shows the trace of the fault. No vertical exaggeration. b) Cross section north of the previous one. Same characteristics as (a).

deformed zone to the east. These two fault systems are gathered south of 11.5°S to form only one.

In the eastern sub-Andes, some events have been located. Since they are far from the seismic array, only events of relatively large magnitude were recorded by enough stations to be located, and among them only the deepest ones passed the selection criteria. Thus, the overall picture is biased. Nevertheless, some epicenters may be related to the main geological faults mapped from SLAR imagery.

State of Stress

Fifty-six events with a total amount of more than 600 polarities of first P-wave motion have been used to determine the orientation and shape factor of the stress tensor (Fig. 8) using the method developed by Rivera and Cisternas (1990). The focal mechanisms presented in Figs. 6 and 7 are a by-product of the method. Generally the number of polarities is not sufficient to identify one of the two focal planes as the fault plane, as this method is potentially able to do. 92% of the polarities are explained by a single stress tensor, and the likelihood, which takes into account the distance from the polarity to the nodal plane, is 0.95. The maximum principal stress is horizontal and

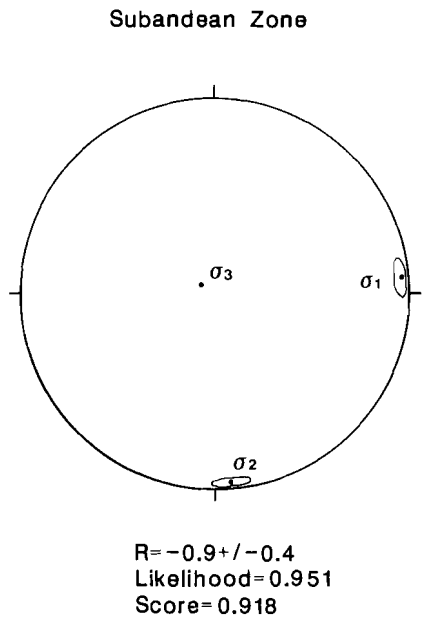

Fig. 8. Stress tensor for the sub-Andean zone deduced from the inversion of polarities of first arrivals. Lower hemisphere projection (Rivera and Cisternas, 1990).

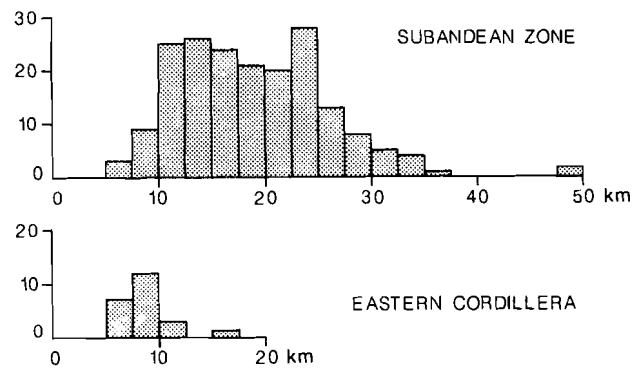

Fig. 9. Distribution of depths for the most reliable events (TMRCRU) in the sub-Andean zone and in the Eastern Cordillera.

strikes 85°E; the minimum one is nearly vertical. The direction of the compression is, therefore, very close to that of the convergence between the Nazca plate and the South American plate, about 80° according to Minster and Jordan (1978). The shape factor, $R = \sigma_1 - \sigma_2 / \sigma_2 - \sigma_3 = -0.9$, indicates a strong compressive regime.

Depths of Foci

One very peculiar feature of the crustal seismicity in the sub-Andean zone is the great depth of the hypocenters in comparison with other active regions in the world. Suarez *et al.* (1983) and Suarez *et al.* (1990) assert that the whole crust may be affected by faulting; however, in both studies determination of the depths is not of the best quality according to the authors. We present in Fig. 9 the distribution of the most reliable hypocentral (MRH) depths for the sub-Andean zone and the Eastern Cordillera. In the latter case, faulting affects only the upper part of the crust. In strong contrast, in the sub-Andean zone, 42% of the events occurred at depths greater than 20 km, 10% at depths greater than 30 km and up to 35 km.

Because the depth of the Moho is unknown, it is not possible to conclude that the whole crust has a fragile behavior, but our results strongly confirm that at least most of the crust, including its lower part, is brittle. As assumed before, this observation may be related to the underthrusting of the Brazilian Shield along the west-dipping fault previously set up, so that cold material of the upper crust is buried.

Two events occurred inside the network at depths close to 50 km, nearly at the vertex of the boundary between the high chain and the lowlands (Fig. 6). Several attempts with different velocity models lead to close solutions. Four other events were located at depths greater than 40 km, but they belong to the RH set, so that their depth is not as well constrained as the first two. As there is no well determined activity between 35 km and 50 km (Fig. 9), it is tempting to postulate that these events take place in the upper mantle, which may be fragile under some conditions (Chen and Molnar, 1983). It is not the only region where such an observation is reported. In the Tian Shan, where the crust is being shortened along steeply dipping inverse faults in a way very similar to that which we observe in the sub-Andean zone, at least one well located event occurred between 40 and 50 km (Molnar and Chen, 1982).

MECHANISMS OF MAJOR EARTHQUAKES SINCE 1947

In this section we present focal mechanisms of the main earthquakes that occurred in the sub-Andean region of central Peru, determined using the method developed by Jimenez *et al.* (1989) (Fig. 10). In this method focal mechanisms are determined by the analysis of three components: surface waves of single station records, by inversion of the source phase, and amplitude spectra in terms of the seismic moment tensor components.

The first well documented earthquake in the area under study occurred on November 1, 1947. Its epicenter, 11°S, 75°W according to USCGS, is situated within the main zone of activity we observed during the 1985 field experiment. The magnitude of this event was M_S=7.5 (USGS), and it is thought to be the greatest event in the region. Damage was particularly noticeable in Satipo, and the area of maximum intensity (IX M.M.) is just to the southeast of the calculated epicenter (Silgado, 1948). Goller (1949) studied the aftershocks recorded at the Huancayo observatory; he determined their distances using S-P times and their azimuth from the P-wave polarization. His results are shown on Fig. 10. The epicenters lie east of the main shock location and of the seismic activity observed during our field work; this discrepancy probably results from the velocity model

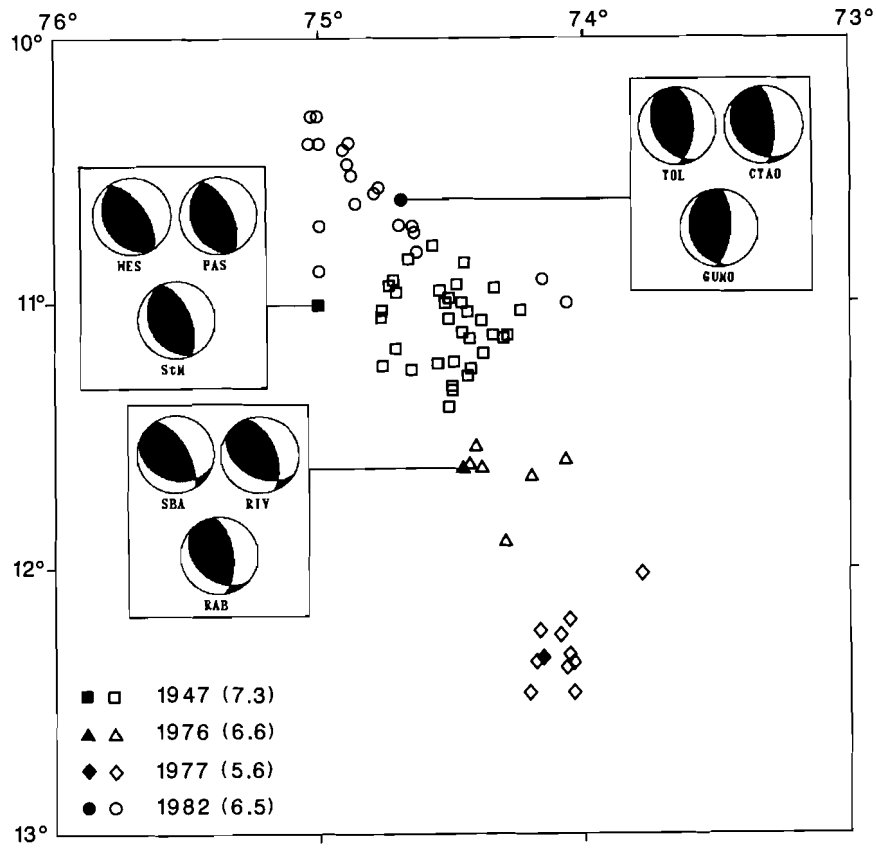

Fig. 10. Main shocks (closed symbols) and their respective aftershocks sequences (open symbols) since 1947 (1947 from Goller, others from ISC). Insets display focal mechanisms from single station inversion (Jimenez *et al.*, 1989).

used by Goller and from errors inherent in his method.

To determine the focal mechanism of this event, we used records from Weston (WES, USA), Pasadena (PAS, USA) and Saint Maur (PAR, France). Purely inverse dip-slip faulting is found on a plane striking about N155° and dipping about 30° (Fig. 10). This last value seems to be too small compared with the dips we observed previously (*cf.* Fig. 7a), and it will be the same for the two following events without any obvious reason to explain this discrepancy. The depth is calculated at 22 km, which is rather shallow for the region. The moment, between 5 and 8.5×10^{26} dyne.cm, corresponds to a magnitude $M_W=7.1$ to 7.2, a value close to that of Gutenberg and Richter (1954) and Abe (1981), both of whom give a magnitude of 7.3 for this event.

The second event we studied occurred on May 15, 1976, at 11.62°S, 74.45°W, and at a depth of 5 km following ISC, with a magnitude $M_S=6.6$ (NEIS). ISC located only a few aftershocks following this event. The aftershock zone is contiguous to that of the 1947 earthquake but poorly defined. The focal mechanism was determined from the records obtained from Scott Base (SBA, Antarctica), Riverview (RIV, Australia), and Rabaul (RAB, New Britain). It corresponds to an inverse fault with a small sinistral strike-slip component if the plane dipping to the southwest is taken as fault-plane. This strikes N115° and dips 37°, a value close to that expected from microseismicity results. The 17-km depth of the hypocenter is a value more realistic than the 5 km given by the ISC. The seismic moment, 5×10^{26} dyne.cm, corresponds to a magnitude $M_W=7.1$. This value is significantly higher than that given by NEIS; however, the two stations where the calculation of the seismic moment was possible indicate the same value.

The earthquake of March 8, 1977 ($M_S=5.6$) was located to the south of the previous one, but it was impossible to obtain its mechanism due to poor signal to noise ratio.

Finally, we studied the November 19, 1982 earthquake, which was situated in the northern part of the region: 10.61°S, 74.69°W from ISC. The inversion of the data from Toledo (TOL, Spain), Charters Tower (CTAO, Australia), and Guam (GUMO, Marianas Islands) leads to an inverse mechanism with a very small sinistral component of strike-slip. The fault plane strikes about N150° and dips 30° to the southwest. This solution is quite comparable to the focal mechanism obtained by the NEIS from first motion (PDE) and to that of Dziewonski *et al.* (1983). The aftershock zone (from ISC bulletins) depicts an elongated cluster about 50 km long to the north of the 1947 one. We calculated a seismic moment ranging from 0.7 to 2×10^{26} dyne.cm, thus a magnitude M_W between 6.5 and 6.8, in agreement with M_S.

The overall picture given by the major earthquakes and their aftershocks is quite comparable to that produced by the microearthquake survey (see

Figs. 5 and 10), although the belt of activity at the boundary between the Eastern Cordillera and the sub-Andean zone north of 11°S is not indicated by teleseismic data. Among the two parallel branches where seismic activity concentrates in this part of the area (see Fig. 5), it is by far the weakest. The two observations converge, but it cannot be asserted that any big earthquake could not occur there. The main shock and aftershock sequence of 1982 are about 25 km to the east of the branch defined by microearthquakes; however, the relocation by Dziewonski *et al.* of this earthquake places the epicenter 0.25° westward, *i.e.*, within the active belt of the 1985 survey. Such an error of epicentral position by ISC is not unusual in this portion of the Andes (Dorbath *et al.*, 1990). Using the Dziewonski *et al.* location and the distribution of activity determined by our network, the teleseismically located major earthquake and the following aftershock sequence are in fairly good agreement, the latter being, of course, more scattered. One may conclude that most of the major earthquakes in this area occur on the fault bordering the high chain south of 11°S and its direct prolongation to the north. Therefore, both microseismic activity and major earthquakes take place on a single narrow fault system that appears to be the main tectonic feature in the region.

DISCUSSION

The configuration of the network warrants reliable depth determinations, at least for events belonging to the MRH set. The distribution of events with depth (see Fig. 9) in the sub-Andes shows that even if the whole crust is not involved in the shortening process, at least a large part of the lower crust is. This style of deformation, prevailing in the western part of the sub-Andes where depths are well controlled, is in strong contrast with the thin-skin tectonics documented in southern Peru, Bolivia, and northern Argentina (Allmendinger *et al.*, 1983; Martinez and Tomasi, 1978; Martinez, 1980), where the Altiplano becomes the major feature of the chain. More to the east, the seismicity, sparse and far from the array, does not allow us to generalize the thick-skin tectonic deformation process to the entire sub-Andean belt. Moreover, the studies made by Ham and Herrera (1963) as well as Pardo (1982) suggest thin-skin tectonics along a décollement that may connect to the western fault systems.

Our microseismic study reveals two active fault systems, at the boundary between the Eastern Cordillera and the sub-Andes and within the sub-Andes. South of 11°S, these two systems gather to form only one along the boundary. North of 11°S, they are parallel, a few tens of km apart. The faults dip westward at angles of about 45°. Focal mechanisms of microearthquakes, as with major shocks, are mostly inverse dip-slip faulting. The consequence of such movement is the uplift of the Eastern Cordillera along its east-bordering fault and, north of 11°S, the uplift of a western sub-Andean block between the two fault systems. This last uplift can be noticed on topographic maps (see Fig. 5); here, extensional stress due to the increasing elevation compensates compressive stress, and the amount of activity decreases on the bordering fault. This assumption is in agreement with the low activity observed along the boundary fault at these latitudes. The process just described leads to the widening of the chain toward the east in such a manner that the 11°S topographic offset will progressively be removed.

It is well known that the shallow seismic activity is very weak within the sub-Andean zone of southern Peru and northern Bolivia (Jordan *et al.*, 1983), *i.e.*, along the widest part of the chain where the Altiplano is present. In Peru, the most seismically active area occurs between 9° and 13°S. Thus, the tectonic process we proposed before leads to widening of the chain immediately north of the segment, where the chain is already very wide. In the southern extremity of the Altiplano, the chain again strongly narrows and intense seismic activity is also found, with a thick-skin tectonic style similar to that which we observed in central Peru and in a symmetric position relative to the Altiplano (Jordan *et al.*, 1983; Smalley and Isacks, 1990). It must be emphasized that these two zones where the width of the chain abruptly changes, in central Peru and northern Argentina, roughly correspond to changes in the slab shape. Between these two deflections, the subduction is "normal" with a constant 30° dip, whereas north and south it is subhorizontal at a depth of 80-100 km (Grange *et al.*, 1984; Jordan *et al.*, 1983). Therefore, at both extremities of the Altiplano, the sub-Andean zone is a zone of intense deformation where western sub-Andean blocks are uplifted and accreted to the Eastern Cordillera.

During the last 50 years, the complete segment between 10.5°S and 12.5°S has been broken by large earthquakes (Fig. 10). Therefore, recurrence times for these earthquakes should not be much larger than this time interval, because otherwise, the probability for this segment being entirely broken during this time interval would be very small. Since all the earthquakes have taken place on the same fault system, Brune's (1968) approach is sufficient to compute the rate of deformation. If S_i and d_i are, respectively, the ruptured surface and the slip during the event i, then:

$$\Sigma S_i d_i = \frac{1}{\mu} \Sigma M_{oi}$$

where M_{oi} is the static seismic moment. The mean slip distributed on the complete surface S is:

$$\bar{d} = \frac{\Sigma S_i d_i}{S} = \frac{1}{\mu} \frac{\Sigma M_{oi}}{S}$$

and

$$\dot{\bar{d}} = \frac{1}{\mu} \frac{\Sigma M_{oi}}{S \Delta t}$$

For the time interval and the segment under consideration, we find the mean slip is 30 cm and the rate of shortening is 6 mm/year. Thus the shortening is about 4 mm/year if taking 45° as the dip of the fault. This is about two times the value calculated by Suarez *et al.* (1983). The difference may result in the fact that these authors took into account a much larger area, including different segments of the chain.

The present shape of the subducted slab in central Peru probably was initiated 5 to 6 Ma, when volcanism stopped (Sébrier *et al.*, 1988). With the rate of shortening calculated above, this period of time corresponds to an amount of 20 km of shortening. Northward, Pardo (1982) found that shortening during Pliocene reaches about 30 km. This value includes deformation in the eastern part of the sub-Andean zone, where, however, it is less important. Therefore, in central Peru, most of the shortening of the western part of the sub-Andean zone occurs following the tectonic process described previously.

CONCLUSION

The seismicity in the eastern high Andes of central Peru is essentially concentrated around the Mantaro Basin (Dorbath *et al.*, 1990).

An intense seismic belt underlies the transition from the Eastern Cordillera to the lowlands, between 10.5°S and 11.5°S. Here also took place the 1947 major earthquake (M_S=7.3). This seismicity can be associated with an inverse dip-slip fault striking N140° and steeply dipping to the west. Well controlled hypocentral depths are found up to 35 km, which is particularly deep for crustal seismicity and may indicate the presence of cold material resulting from the underthrusting of the Brazilian Shield.

The most active seismic band does not follow the entire border between the high chain and the lowlands; north of 11°S, where this boundary shifted toward the west, it goes on into the same azimuth. As a consequence, the region between this major active fault and the border of the Eastern Cordillera is uplifted. This process leads to a widening of the Andes on their eastern side toward the north; it is symmetric to what is observed in Argentina south of the widest part of the Andes, where the Altiplano is present. However, this dynamic process is more developed in Argentina (Jordan *et al.*, 1983).

Finally, the amount of shortening in the western sub-Andes deduced from the study of major earthquakes that occurred during the past 50 years is estimated to be about 4 mm/year.

Acknowledgements—This work is part of a French-Peruvian cooperative project between the Institut Français de Rechereche Scientifique pour le Developpement en Cooperation (ORSTOM) and the Instituto Geofísico del Perú (IGP). We wish to thank the following for their assistance during the field work: M. Chang, O. Veliz, J. Tavera, M. Morales, J. Berospi, M. Diament, H. Arjono, and A. S. de Biévre. Financial support was provided by ORSTOM and INSU.

REFERENCES

Abe, K., 1981. Magnitudes of large shallow earthquakes from 1904 to 1980. *Physics of the Earth and Planetary Interiors* **27**, 72–92.

Allmendinger, R. W., Ramos, V. A., Jordan, T. E., Palma, M., and Isacks, B. L., 1983. Paleogeography and Andean structural geometry, northwest Argentina. *Tectonics* **2**, 1–16.

Audebaud, E., Capdevilla, R., Dalmayrac, B., Debelmas, J., Laubacher, G., Lefevre, C., Marocco, R., Martinez, C., Mattauer, M., Mégard, F., Paredes, J., and Tomasi, P., 1973. Les traits géologiques essentiels des Andes Centrales (Pérou-Bolivie). *Revue de Géographie Physique de Géologie Dynamique* **15**, 73–114.

Blanc, J. L., 1984. *Etude Néotectonique et Sismotectonique des Andes du Pérou Central dans la Région de Huancayo.* Thèse 3° Cycle, Université Paris Sud, France, 201 p.

Blanc, J. L., Sébrier, M., and Cabrera, J., 1983. Estudio microtectonico de la falla sismica de Huaytapallana (Andes del Peru Central). *Revista Geofisica IPGH, Mexico* **18/19**, 5–24.

Brune, J. N., 1968. Seismic moment, seismicity and rate of slip along major fault zones. *Journal of Geophysical Research* **73**, 777, 784.

Chen, W. P., and Molnar, P., 1983. The depth distribution of intracontinental and intraplate earthquakes and its implications for the thermal and mechanical properties of the lithosphere. *Journal of Geophysical Research* **88**, 4183–4214.

Dalmayrac, B., and Molnar, P., 1981. Parallel thrusts and normal faulting in Peru and constraints on the state of stress. *Earth and Planetary Science Letters* **55**, 473–481.

Deverchère, J., Dorbath, C., and Dorbath, L., 1989. Extension related to a high topography: Results from a microearthquake survey in the Andes of Peru and tectonic implications. *Geophysical Journal International* **98**, 281–292.

Dorbath, C., Dorbath, L., Cisternas, A., Deverchere, J., Diament, M., Ocola, L., and Morales, M., 1986. On crustal seismicity of the amazonian foothill of the central peruvian Andes. *Geophysical Research Letters* **13**, 1023–1026.

Dorbath, C., Dorbath, L., Cisternas, A., Deverchère, J., and Sébrier, M., 1990. Seismicity of the Huancayo Basin (Central Peru) and the Huaytapallana Fault. *Journal of South American Earth Sciences* **3**, 21–29.

Doser, D. I., 1987. The Ancash, Peru, earthquake of 1946 November 10: Evidence for low-angle normal faulting in the high Andes of northern Peru. *Geophysical Journal, Royal Astronomical Society* **91**, 57–71.

Durand, P., 1987. *La Sismicité en Equateur: Programme de Localisation et Traitement des Données.* Diplome d'Ingénieur, Université Louis Pasteur, Strasbourg, France, 298 p.

Dziewonski, A. M., Friedman, A., Giardini, D., and Woodhouse, J. H., 1983. Global seismicity of 1982: Centroid-moment tensor solutions for 308 earthquakes. *Physics of the Earth and Planetary Interiors* **33**, 76–90.

Goller, H., 1949. El terremoto del 1° de Noviembre de 1947 en Satipo. *Boletin de la Sociedad Geológica del Perú* **22**, 1–4.

Grange, F., 1983. *Etude Sismotectonique détaillée de la Subduction Lithosphérique au Sud Pérou.* Thèse 3° Cycle, Université des Sciences Medicin, Grenoble, France, 170 p.

Grange, F., Hatzfeld, D., Cunningham, P., Molnar, P., Roecker, S. W., Suarez, G., Rodrigues, A., and Ocola, A. L., 1984. Tectonic implications of the microearthquake seismicity and fault plane solutions in southern Peru. *Journal of Geophysical Research* **89**, 6139–6152.

Gutenberg, B., and Richter, C. F., 1954. *Seismicity of the Earth and Associated Phenomena.* Princeton University Press, Princeton, NJ, USA, 310 p.

Ham, C. K., and Herrera, L. J., 1963. Role of sub-Andean fault system in tectonics of eastern Peru and Ecuador. In: *Backbone of the Americas* (edited by O. Childs and B. W. Beebe). American Association of Petroleum Geologists, Memoir **2**, 47–61.

Isacks, B. L., and Barazangi, M., 1977. Geometry of Benioff zones: Lateral segmentation and downward bending of the subducted lithosphere. In: *Island Arcs, Deep Sea Trenches and Back-Arc Basins, Vol. 1* (edited by M. Ewing), pp. 99–114. American Geophysical Union, Geodynamics Series, Washington, DC, USA.

Jimenez, E., Cara, M., and Rouland, D., 1989. Focal mechanisms of moderate-size earthquakes from the analysis of single-station three-component surface-wave records. *Bulletin of the Seismological Society of America* **79** (4), 955–972.

Jordan, T. E., Isacks, B. L., Allmendinger, R. W., Brewer, J. A., Ramos, V. A., and Ando, C. J., 1983. Andean tectonics related to geometry of subducted Nazca plate. *Bulletin of the Geological Society of America* **94**, 341–361.

Klein, F. W., 1978. *Hypocenter Location Program* HYPOINVERSE. U.S. Geological Survey, Open File Report **78-694**, 113 p.

Martinez, C., 1980. *Geologie des Andes Boliviennes.* Travaux et Documents, ORSTOM **119**, 351 p.

Martinez, C., and Tomasi, P., 1978. *Carte Structurale des Andes Septentrionales de Bolivie au 1/1 000 000.* ORSTOM, Paris.

Mégard, F., 1978. *Etude Géologique des Andes du Pérou Central.* ORSTOM, Mémoire **86**, 310 p.

Meissner, R. O., Flueh, E. R., Stibane, C., and Berg, E., 1976. Dynamic of the active plate boundary in southwest Colombia according to recent geophysical measurements. *Tectonophysics* **35**, 115–136.

Mingramm, A., Russo, A., Pozzo, A., and Cazau, L., 1979. Sierras Subandinas. *I Simposio de Geológica Regional Argentina*, pp. 95–138. Academía Nacional Ciencas, Córdoba, Argentina.

Minster, J. B., and Jordan, T. H., 1978. Present-day plate motion. *Journal of Geophysical Research* **83**, 5331–5354.

Molnar, P., and Chen, W. P., 1982. Seismicity and mountain building. In: *Mountain Building Processes* (edited by K. J. Hsü), pp. 41–57. Academic Press, London, England, UK.

Ocola, L. C., and Meyer, R.P., 1973. Crustal structure from the Pacific basin to the Brazilian Shield between 12° and 30° south latitude. *Bulletin of the Seismological Society of America* **84**, 3387–3403.

Ocola, L. C., Meyer, R. P., and Aldrich, L. T., 1971. Gross crustal structure under Bolivian Altiplano. *Earthquake Notes* **42**, 33–48.

Pardo, A., 1982. *Caracteristicas Estructurales de la Faja Subandina del Norte del Peru.* Departamento de Geología, Petroleos del Peru SA, Lima, 16 p.

Philip, H., and Mégard, F., 1977. Structural analysis of the superficial deformation of the 1969 Pariahuanca earthquakes (central Peru). *Tectonophysics* **38**, 259–278.

Rivera, L., and Cisternas, A., 1990. Stress tensor and fault plane solutions for a population of earthquakes. *Bulletin of the Seismological Society of America* **80** (3), 600–614.

Sébrier, M., Mercier, J. L., Macharé, J., Bonnot, D., Cabrera, J., and Blanc, J. L., 1988. The state of stress in an overriding plate situated above a flat slab: The Andes of central Peru. *Tectonics* **7**, 895–928.

Sébrier, M., Mercier, J. L., Mégard, F., Laubacher, G., and Carey-Gailhardis, E., 1985. Quaternary normal and reverse faulting and the state of stress in the central Andes of south Peru. *Tectonics* **7**, 739–780.

Silgado, E., 1948. Datos sismológicos del Perú 1947. *Boletin de Instituto Geológico Perú* **11**, 25–31.

Silgado, E.,1951. The Ancash, Peru, earthquake of November 10, 1946. *Bulletin of the Seismological Society of America* **41**, 83–100.

Smalley, R., Jr., and Isacks, B. L., 1990. Seismotectonics of thin and thick-skinned deformation in the Andean foreland from local network data: Evidence for a seismogenic lower crust. *Journal of Geophysical Research*, in press.

Suarez, G., Gagnepain, J., Cisternas, A., Hatzfeld, D., Molnar, P., Ocola, L., Roecker, S. W., and Viodé, J. P., 1990. Tectonic deformation of the Andes and the configuration of the subducted slab in central Peru: Results from a micro-seismic experiment. *Geophysical Journal International*, in press.

Suarez, G., Molnar, P., and Burchfield, B. C., 1983. Seismicity, fault-plane solutions, depth of faulting, and active tectonics of the Andes of Peru, Ecuador and southern Colombia. *Journal of Geophysical Research* **88**, 10403–10428.